Thermodynamics and Structures of Nickel(II) Chloro Complexes in *N,N*-Dimethylacetamide

Honoh Suzuki and Shin-ichi Ishiguro*

Department of Electronic Chemistry, Tokyo Institute of Technology at Nagatsuta, 4259 Nagatsuta, Midori-ku, Yokohama 227, Japan

Received April 1, 1992

Formation of nickel(II) chloro complexes in *N,N*-dimethylacetamide (DMA) has been studied by spectrophotometry at 278, 298, and 318 K and by calorimetry at 298 and 318 K. Formation constants, reaction enthalpies and entropies, and electronic spectra for four mononuclear complexes $[NiCl_n]^{(2-n)+}$ (n = 1–4) have been determined at each temperature. The obtained spectra indicate an octahedral geometry for $[Ni(DMA)_6]^{2+}$ and tetrahedral ones for $[NiCl_3(DMA)]^-$ and $[NiCl_4]^{2-}$. The $[NiCl]^+$ complex, however, shows a distinct absorption at 461 nm, and $[NiCl_2]$ shows one at 489 nm, which are markedly different from those in similar donor solvents such as *N,N*-dimethylformamide (DMF). These two complexes are strongly thermochromic, suggesting that the following equilibria may hold for the mono- and dichloro complexes: $[NiCl(DMA)_5]^+ \rightleftarrows [NiCl(DMA)_4]^+ + DMA$ and $[NiCl_2(DMA)_3] \rightleftarrows [NiCl_2(DMA)_2] + DMA$. Overall formation of $[NiCl_4]^{2-}$ is strongly favored and much less endothermic in DMA than in DMF. The stepwise ΔH_n° and ΔS_n° values (n = 1, 2) are larger in DMA, being consistent with the strong desolvation in earlier steps of complexation. The molar heat capacity of complexation, ΔC_{pn}°, estimated from temperature dependence of ΔH_n° and ΔS_n°, is positive for n = 1 and negative for n = 3, which is attributed to the shift of the solvation equilibria with temperature. These results indicate that steric requirements of the acetyl methyl groups of DMA molecules coordinated to the nickel(II) ion lead to (i) weaker solvation and thus more favored complexation and (ii) formation of the unusual coordination structures, five-coordinate $[NiCl(DMA)_4]^+$ and $[NiCl_2(DMA)_3]$ and tetrahedral $[NiCl_2(DMA)_2]$.

Introduction

N,N-Dimethylacetamide (DMA) is a fairly strong donor solvent with a molecular structure analogous to that of *N,N*-dimethylformamide (DMF). They have similar physicochemical properties, such as dielectric constants, donor numbers, and acceptor numbers (DMA, ϵ = 37.8, D_N = 27.8, A_N = 13.6; DMF, ϵ = 36.7, D_N = 26.6, A_N = 16.0).[1,2] In both solvents, the nickel(II) ion is hexasolvated via the carbonyl oxygens, showing typical d–d transition spectra of the octahedral coordination structure.[3] The D_q value for $[Ni(DMA)_6]^{2+}$ (769 cm^{-1}) is, however, considerably smaller than that for $[Ni(DMF)_6]^{2+}$ (850 cm^{-1}); this is unexpected from the similar donor properties, and thus attributed to a steric repulsion between acetyl methyl groups of neighboring DMA molecules in the first solvation shell.[4] A solution NMR study shows that solvation of metal ions is weaker and solvent exchange much faster in DMA than in DMF.[5] In the crystal of $[Cu(ClO_4)_2(DMA)_4]$, in which DMA molecules equatorially coordinate, two of the Cu–O–C–N torsion angles indeed deviate largely from 180°,[6] whereas in analogous DMF solvates the metal–O–C–N torsion angles are close to 180°.[7,8]

Steric constraint of solvent molecules coordinating a metal ion often plays a crucial role in complexation reactions. In a very bulky donor solvent, hexamethylphosphoric triamide (HMPA), bivalent transition metal ions are coordinated with only four solvent molecules, and their halogeno complexes are much more stable than those in DMF.[9] This has drawn our particular attention to the thermodynamics and structures of metal complexes in DMA. Precise thermodynamic studies on complexation are very few in DMA, and little is known about the solvent effect of DMA on complexation equilibria. In this paper, we report a spectrophotometric and calorimetric investigation of nickel(II) chloro complexes in DMA. In DMF, our previous study[10] showed that four mononuclear nickel(II) chloro complexes are formed, the coordination geometry of which varies from octahedral complexes, $[Ni(DMF)_6]^{2+}$, $[NiCl(DMF)_5]^+$, and $[NiCl_2(DMF)_4]$, to tetrahedral ones, $[NiCl_3(DMF)]^-$ and $[NiCl_4]^{2-}$. In DMA, however, we have found markedly different structures and stabilities of complexes compared to those in DMF.

Experimental Section

Materials. All chemicals were of reagent grade. The DMA solvate of nickel(II) tetrafluoroborate, $Ni(BF_4)_2 \cdot x$DMA, was prepared by dissolving the relevant hydrate in DMA and removing water and excess DMA in a rotary evaporator below 70 °C. The hygroscopic yellow crystals were recrystallized from DMA and dried in vacuo over P_2O_5 at room temperature. (*Caution*! Contact with fingers and nails should be avoided, because the fluoride ion might be present due to thermal decomposition or hydrolysis.) Analysis of the nickel ion by EDTA titrations[11] showed x = 5.9 for the crystals finally obtained. Tetraethylammonium tetrafluoroborate and tetra-*n*-butylammonium tetrafluoroborate were prepared and purified according to the literature.[12] Tetra-*n*-butylammonium chloride (Tokyo Kasei) was dried at 45 °C in vacuum and promptly used without further purification. DMA was dried with BaO for several days, refluxed with BaO for 2 h, then distilled under a reduced pressure (49 °C/1.3 kPa), and kept in a drybox over P_2O_5.[13] Other chemicals were purified as described elsewhere.[10]

(1) Riddick, J. A.; Bunger, W. B.; Sakano, T. K. *Organic Solvents*, 4th ed.; Wiley-Interscience: New York, 1986.
(2) Gutmann, V. *The Donor-Acceptor Approach to Molecular Interactions*; Plenum: New York and London, 1978.
(3) Lever, A. P. B. *Inorganic Electronic Spectroscopy*, 2nd ed.; Elsevier: Amsterdam, 1984.
(4) Drago, R. S.; Meek, D. W.; Joesten, M. D.; LaRoche, L. *Inorg. Chem.* **1963**, *2*, 124.
(5) Lincoln, S. F.; Hounslow, A. M.; Boffa, A. N. *Inorg. Chem.* **1986**, *25*, 1038.
(6) Lemoine, P.; Herpin, P. *Acta Crystallogr.* **1980**, *B36*, 2772.
(7) Young, A. C. M.; Walters, M. A.; Dewan, J. C. *Acta Crystallogr.* **1989**, *C45*, 1733.
(8) Tsintsadze, G. V.; Porai-Koshits, M. A.; Antsyshkina, A. S. *Zh. Strukt. Khim.* **1967**, *8*, 296; *J. Struct. Chem.* (*Engl. Transl.*) **1967**, *8*, 253.
(9) Abe, Y.; Ozutsumi, K.; Ishiguro, S. *J. Chem. Soc., Faraday Trans. 1* **1989**, *85*, 3747.
(10) Ishiguro, S.; Ozutsumi, K.; Ohtaki, H. *Bull. Chem. Soc. Jpn.* **1987**, *60*, 531.
(11) Bassett, J.; Denney, R. C.; Jeffery, G. H.; Mendham, J. *Vogel's Textbook of Quantitative Inorganic Analysis*, 4th ed.; Longman: London, 1978.
(12) Sawyer, D. T.; Roberts, J. L., Jr. *Experimental Electrochemistry for Chemists*; Wiley-Interscience: New York, 1974.
(13) Schmulbach, C. D.; Drago, R. S. *J. Am. Chem. Soc.* **1960**, *82*, 4484.

0020-1669/92/1331-4178$03.00/0

Measurements. Electronic spectra of nickel(II) chloride–DMA solutions were recorded with a Hitachi 340 spectrophotometer. A quartz flow cell with a path length of 1.0 cm was connected to a reaction vessel through Teflon tubes and a Teflon flow pump. The cell and the vessel were jacketed and kept at a constant temperature (278, 298, or 318 K) within ±0.2 K by circulating water. An $Ni(BF_4)_2$–DMA solution of 20–40 cm^3 was introduced into the vessel and titrated with a 0.1 mol dm^{-3} $(n\text{-}C_4H_9)_4NCl$ solution under an argon atmosphere. All metal solutions contained 0.1 mol dm^{-3} $(n\text{-}C_4H_9)_4NBF_4$ as a constant ionic medium, and the initial metal concentrations were varied in the range 10–30 mmol dm^{-3}. Absorbance data at 50 different wavelengths were collected and analyzed.

Calorimetric titrations were carried out in a twin-type isoperibol calorimeter (Tokyo Riko) regulated at a constant temperature (298 or 318 K) within ±0.0001 K. An ionic medium of either 0.1 mol dm^{-3} $(n\text{-}C_4H_9)_4NBF_4$ or 0.1 mol dm^{-3} $(C_2H_5)_4NBF_4$ was used. An $Ni(BF_4)_2$–DMA solution of 2.5–20 mmol dm^{-3} (20 cm^3) was titrated with a 0.1 mol dm^{-3} $(n\text{-}C_4H_9)_4NCl$ or $(C_2H_5)_4NCl$ solution under an argon atmosphere. An autoburet containing the titrant was placed in a room at 298 K and connected to the titration outlet through a 15-m-length Teflon tube, which was coiled round an aluminum block inside the calorimeter. A slow titration speed (less than 0.05 cm^3 s^{-1}) allowed a complete thermal equilibration of the titrant before its introduction into the vessel, which was verified by blank titration and gravimetric calibration. Heats of complexation at each titration point ranged from −2.5 to +0.8 J with an average 3σ of 0.012 J. Heats of dilution, separately measured by titrating a metal-free ionic medium solution with the titrant, were found to be less than 0.05 J and were used for correction of reaction heats.

All solutions were prepared in a drybox over P_2O_5 at 298 K, and their volumes and concentrations at 278 and 318 K were calculated from density changes determined separately.

Data Analysis. Observed absorbances and reaction heats were analyzed by considering the following complexation equilibria:

$$Ni^{2+} + nCl^- \rightleftarrows [NiCl_n]^{(2-n)+} \qquad (n = 1, ..., N_{max}) \qquad (1)$$

At the ith titration point, total concentrations of nickel and chloride ions, $C_{M,i}$ and $C_{X,i}$, are expressed as

$$C_{M,i} = [M]_i + \sum \beta_n [M]_i [X]_i^n \qquad (2)$$

$$C_{X,i} = [X]_i + \sum n\beta_n [M]_i [X]_i^n \qquad (3)$$

where $[M]_i$ and $[X]_i$ denote the concentrations of free metal and ligand ions, respectively, and β_n denotes the overall formation constant of $[NiCl_n]^{(2-n)+}$. An absorbance of the ith solution at the jth wavelength, $A_{ij,calcd}$, is calculated from the Lambert–Beer law:

$$A_{ij,calcd} = d(\epsilon_{j0}[M]_i + \sum \epsilon_{jn}\beta_n [M]_i [X]_i^n) \qquad (4)$$

where d denotes the path length and ϵ_{j0} and ϵ_{jn} are the molar extinction coefficients of Ni^{2+} and $[NiCl_n]^{(2-n)+}$, respectively, at the jth wavelength. Formation constants and molar extinction coefficients were simultaneously determined by minimizing the error-square sum $U = \sum(A_{ij,calcd} - A_{ij,obsd})^2$.

Numerical procedures were performed with a PC9801VM microcomputer (NEC) and a FORTRAN77 program MQSPEC written by us (source code is available upon request).[14] In eq 4, once the formation constants are assumed, the absorbances are linearly dependent on the extinction coefficients. Accordingly, optimization for ϵ's does not require any iteration procedure or initial guesses; a unique solution for the whole ϵ set can be obtained readily by the standard linear least-squares method. This greatly simplifies solution search in MQSPEC, in which only the formation constants are treated as unknown variables during the nonlinear optimization process. All the parameters (β's and ϵ's) are treated as independent variables only at the final stage, for the evaluation of standard deviations.

Similarly, a heat of complexation at the ith titration point, $q_{i,calcd}$, is calculated as

$$q_{i,calcd} = -\sum \Delta H^\circ_{\beta n} \beta_n ([M]_i [X]_i^n V_i - [M]_{i-1} [X]_{i-1}^n V_{i-1}) \qquad (5)$$

where $\Delta H^\circ_{\beta n}$ denotes the enthalpy of reaction 1 and V_i the volume of the solution. Formation constants and enthalpies of the complexes were determined by minimizing the error-square sum, $U = \sum(q_{i,calcd} - q_{i,obsd})^2$. A FORTRAN77 program MQCAL was used for optimization.[14]

(14) Suzuki, H. Doctoral Thesis, Tokyo Institute of Technology, Tokyo, 1989.

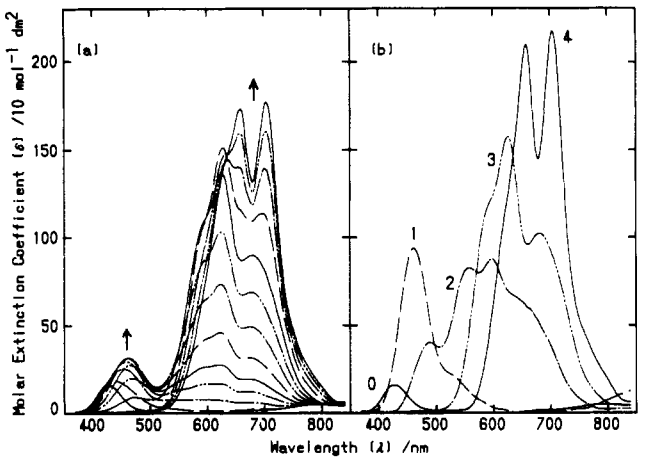

Figure 1. (a) Selected electronic spectra of nickel(II) chloride–DMA solutions at 298 K. The C_X/C_M ratio increased from 0 to 10 as indicated by the arrows. (b) Electronic spectra of individual nickel(II) chloro complexes in DMA at 298 K. The numbers represent n in $[NiCl_n]^{(2-n)+}$.

Table I. Spectrophotometrically Determined Overall Formation Constants, log (β_n/mol^{-n} dm^{3n}), of $[NiCl_n]^{(2-n)+}$ (n = 1–4) in *N*,*N*-Dimethylacetamide Containing 0.1 mol dm^{-3} $(n\text{-}C_4H_9)_4NBF_4$ as a Constant Ionic Medium at T = 278, 298, and 318 K[a]

	298 K				
	(n)[b] = (1–4)	(n) = (1,3,4)	(n) = (2,3,4)	278 K (n) = (1–4)	318 K (n) = (1–4)
log β_1	4.31 (4)	4.5 (2)		4.00 (3)	4.71 (4)
log β_2	8.53 (8)		8.1 (5)	8.03 (7)	9.25 (9)
log β_3	13.0 (1)	13.1 (6)	12.6 (9)	12.67 (9)	13.7 (1)
log β_4	14.8 (1)	15.1 (6)	14.3 (9)	14.45 (9)	15.4 (1)
N[c]	4050	4050	4050	2650	2700
σ_{abs}[d]	0.0025	0.013	0.040	0.0016	0.0018
R[e]	0.0048	0.025	0.076	0.0026	0.0029

[a] Values in parentheses are 3σ in the last significant digits. [b] Complexes considered in the analysis. [c] Number of data points. [d] Standard deviation of the absorbances. [e] Hamilton R factor.

Results

Spectrophotometry. Typical electronic spectra at 298 K are shown in Figure 1a, in which observed absorbances are corrected for dilution, i.e., normalized with the total metal concentration. The solution spectrum of $Ni(BF_4)_2$ has a weak absorption maximum at λ_{max} = 427 nm with a molar extinction coefficient ϵ_{max} = 16 (units: mol^{-1} dm^3 cm^{-1} = 10 mol^{-1} dm^2). Addition of the titrant up to C_X/C_M = 1 raised a new, stronger absorption band at ca. 460 nm, which was not observed in DMF,[10] dimethyl sulfoxide (DMSO),[15] or acetonitrile (MeCN).[16] As the concentration ratio increased to C_X/C_M > 2, the band at 460 nm disappeared and a much stronger absorption occurred over 570–720 nm. A doublet absorption at 658 and 704 nm is characteristic for the distorted tetrahedral complex $[NiCl_4]^{2-}$.[3,17] For C_X/C_M > 3, a clear isosbestic point was observed at 635 nm, which indicated an equilibrium between $[NiCl_3]^-$ and $[NiCl_4]^{2-}$.[18]

A matrix rank analysis[19] indicated the presence of five species, including the solvated Ni^{2+} ion. On this basis, the data were analyzed by considering four mononuclear complexes $[NiCl_n]^{(2-n)+}$ (n = 1–4). The obtained formation constants are shown as set (1–4) in Table I, which satisfactorily reproduced the data with an R factor of 0.5%. We also examined other plausible sets in

(15) Suzuki, H.; Ishiguro, S.; Ohtaki, H. *J. Chem. Soc., Faraday Trans.* **1990**, *86*, 2179.
(16) Suzuki, H.; Ishiguro, S. *Bull. Chem. Soc. Jpn.*, submitted for publication.
(17) Gruen, D. M.; McBeth, R. L. *J. Phys. Chem.* **1959**, *63*, 393.
(18) Nash, C. P.; Jenkins, M. S. *J. Phys. Chem.* **1964**, *68*, 356.
(19) Hugus, Z Z., Jr.; El-Awady, A. A. *J. Phys. Chem.* **1971**, *75*, 2954.

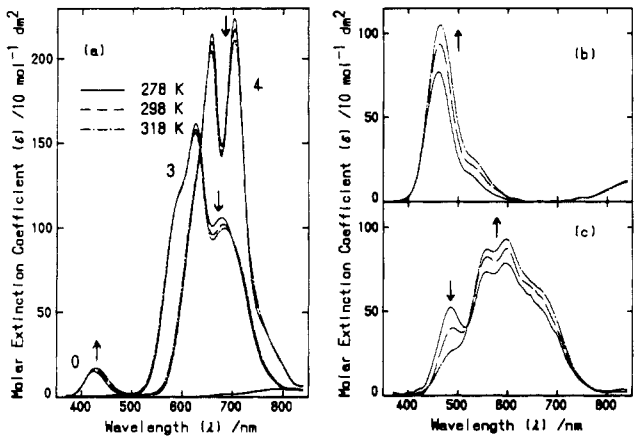

Figure 2. Electronic spectra of individual nickel(II) chloro complexes in DMA at T = 278, 298, and 318 K: (a) Ni^{2+}, $[NiCl_3]^-$, $[NiCl_4]^{2-}$; (b) $[NiCl]^+$; (c) $[NiCl_2]$. The arrows indicate the direction of change with the temperature increase.

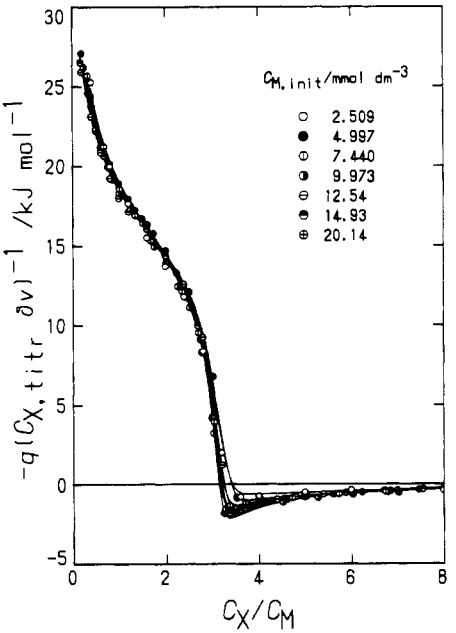

Figure 3. Calorimetric titration curves of nickel(II) chloride–DMA solutions containing 0.1 mol dm^{-3} $(n\text{-}C_4H_9)_4NBF_4$ at 298 K. Initial concentrations of metal ion ($C_{M,init}$/mmol dm^{-3}) are given in the figure. The solid lines were calculated by using the constants in Table II.

which one or more complexes were omitted, but they failed to give a small R value; set (1,3,4) omitting $[NiCl_2]$ and set (2,3,4) omitting $[NiCl]^+$ gave R values of 2.5 and 7.6%, respectively (Table I). Clearly, to account for the observed spectra, all four complexes are indispensable. Electronic spectra of the individual complexes thus determined are shown in Figure 1b.

Solution spectra at 278 and 318 K were similarly analyzed, and the formation constants thus determined are also listed in Table I. Electronic spectra of the individual complexes at these temperatures are compared in Figure 2. The molar extinction coefficients of the complexes were determined with good accuracy at all temperatures, with $3\sigma < 3.3$ for $[NiCl_2]$ and $3\sigma < 1.1$ for the other complexes.

Calorimetry. Calorimetric titration curves obtained in 0.1 mol dm^{-3} $(n\text{-}C_4H_9)_4NBF_4$–DMA at 298 K are shown in Figure 3. In the figure, enthalpies of titration $-q(C_{X,titr}\,\delta v)^{-1}$ are plotted against C_X/C_M, where the symbol $C_{X,titr}$ represents the concentration of chloride ion in the titrant and δv the volume of the titrant added at each titration point.

As the spectrophotometric results indicated the formation of the four mononuclear complexes, we also analyzed the calorimetric

Table II. Overall Formation Constants, log (β_n/mol^{-n} dm^{3n}), and Enthalpies, $\Delta H^\circ_{\beta n}$/kJ mol^{-1}, of $[NiCl_n]^{(2-n)+}$ (n = 1–4) Determined by Calorimetry in *N,N*-Dimethylacetamide Containing 0.1 mol dm^{-3} $(n\text{-}C_4H_9)_4NBF_4$ as a Constant Ionic Medium at T = 298 and 318 K[a]

	298 K			318 K	
	β optmd[b]	β fixed[b]	β optmd[c]	β optmd	β fixed
log β_1	4.1 (3)	4.31	4.4 (6)	4.7 (5)	4.71
log β_2	7.9 (7)	8.53	9 (1)	9 (1)	9.25
log β_3	12.3 (9)	13.0	14 (2)	14 (1)	13.7
log β_4	14 (1)	14.8	16 (2)	15 (2)	15.4
$\Delta H^\circ_{\beta 1}$	28.0 (8)	28.4 (5)	30 (1)	33.4 (7)	32.4 (4)
$\Delta H^\circ_{\beta 2}$	56 (7)	50.4 (7)	55 (10)	53 (1)	52.6 (5)
$\Delta H^\circ_{\beta 3}$	46.9 (3)	47.1 (3)	48.2 (4)	44.5 (3)	44.6 (3)
$\Delta H^\circ_{\beta 4}$	39 (1)	40.7 (5)	44 (1)	37.7 (9)	38.0 (4)
N[d]	160	160	150	148	148
σ_q[e]	0.015	0.017	0.025	0.017	0.020
R[f]	0.020	0.022	0.020	0.018	0.022

[a] Values in parentheses are 3σ in the last significant digits. [b] Key: β optmd, formation constants and enthalpies are simultaneously optimized; β fixed, formation constants are fixed to the values obtained by spectrophotometry (Table I). [c] 0.1 mol dm^{-3} $(C_2H_5)_4NBF_4$ was used as an ionic medium. [d] Number of data points. [e] Standard deviation of the heats (J). [f] Hamilton R factor.

data by considering these complexes. The results are summarized in Table II. When the formation constants and enthalpies were both optimized (noted as "β optmd" in Table II), the heat data were well reproduced with an R factor of 2% and the formation constants obtained were in agreement with those from spectrophotometry within 3σ. The uncertainties of β_n and $\Delta H^\circ_{\beta n}$ were rather large, however. Alternatively, we analyzed the same data by using the formation constants obtained by spectrophotometry as known parameters ("β fixed" in Table II). This resulted in practically the same R value (2.2%) and similar enthalpy values with much smaller 3σ values. Consequently, we took these values as a final choice. The solid lines in Figure 3, which were calculated with these constants, reproduce well the experimental points.

We also carried out calorimetric titrations in 0.1 mol dm^{-3} $(C_2H_5)_4NBF_4$–I MA at 298 K to check the effect of the ionic medium. The result of the analysis is included in Table II. The log β_n values are practically the same as those in 0.1 mol dm^{-3} $(n\text{-}C_4H_9)_4NBF_4$–DMA, but $\Delta H^\circ_{\beta 3}$ and $\Delta H^\circ_{\beta 4}$ are slightly larger. The limited solubility of $(C_2H_5)_4NCl$ in DMA, however, prevented us from obtaining reliable results for the higher complexes in this electrolyte solution.

Calorimetric titration data at 318 K were similarly analyzed, and final values of enthalpies were also determined by using the formation constants obtained from spectrophotometry at 318 K ("β fixed" in Table II).

Thermodynamic parameters, log (K_n/mol^{-1} dm^3), ΔG°_n/kJ mol^{-1}, ΔH°_n/kJ mol^{-1} and ΔS°_n/J K^{-1} mol^{-1}, for the stepwise formation of $[NiCl_n]^{(2-n)+}$ in DMA are summarized in Table III. The table also includes the result of calorimetric titrations in 0.4 mol dm^{-3} $(C_2H_5)_4NClO_4$–DMF at 318 K, which we performed to compare temperature effects on the thermodynamic parameters in DMA and in DMF.

Discussion

Formation constants have been reported for cobalt(II) chloro[20] and bromo[21] complexes and bivalent metal monobromo complexes[22,23] in DMA. To our knowledge, no literature values are presently available for comparison with this work.

Electronic Spectra and Coordination Structures. The peak positions and heights of the obtained spectra are estimated by

(20) Kamieńska, E.; Uruska, I. *Bull. Acad. Pol. Sci., Ser. Sci. Chim.* **1976**, *24*, 567.
(21) Pastewski, R.; Radecki, Z. *Can. J. Spectrosc.* **1989**, *34*, 112.
(22) Strzelecki, H.; Pastewski, R. *Bull. Pol. Acad. Sci., Chem.* **1987**, *35*, 31.
(23) Pastewski, R. *Bull. Pol. Acad. Sci., Chem.* **1988**, *36*, 81.

Table III. Thermodynamic Quantities, log (K_n/mol^{-1} dm^3), ΔG_n°/kJ mol^{-1}, ΔH_n°/kJ mol^{-1}, and ΔS_n°/J K^{-1} mol^{-1}, for the Stepwise Formation of $[NiCl_n]^{(2-n)+}$ in *N,N*-Dimethylacetamide and *N,N*-Dimethylformamide at T = 298 and 318 K[a]

	N,N-dimethylacetamide		*N,N*-dimethylformamide	
	298 K	318 K	298 K[b]	318 K[c]
log K_1	4.31 (4)	4.71 (4)	2.8 (1)	2.85 (7)
log K_2	4.22 (4)	4.54 (5)	0.9 (4)	0.9 (3)
log K_3	4.51 (4)	4.45 (4)	1.8 (5)	2.6 (3)
log K_4	1.73 (1)	1.67 (1)	1.9 (2)	1.70 (8)
ΔG_1°	−24.6 (2)	−28.7 (3)	−16.3 (8)	−17.4 (4)
ΔG_2°	−24.1 (3)	−27.7 (3)	−5 (2)	−5 (2)
ΔG_3°	−25.7 (3)	−27.1 (3)	−10 (3)	−16 (2)
ΔG_4°	−9.87 (5)	−10.17 (5)	−11 (1)	−10.3 (5)
ΔH_1°	28.4 (5)	32.4 (4)	8.6 (6)	9.0 (3)
ΔH_2°	22 (1)	20.3 (7)	19 (16)	25 (12)
ΔH_3°	−3.3 (7)	−8.1 (5)	63 (40)	43 (13)
ΔH_4°	−6.4 (4)	−6.5 (4)	−13 (30)	−5 (3)
ΔS_1°	178 (2)	192 (2)	84 (1)	83 (1)
ΔS_2°	154 (4)	151 (3)	81 (49)	94 (36)
ΔS_3°	75 (3)	60 (2)	245 (125)	186 (39)
ΔS_4°	12 (1)	12 (1)	−9 (97)	17 (8)
$\Delta G_{\beta 4}^\circ$[d]	−84.3 (7)	−93.6 (8)	−42 (1)	−48.7 (7)
$\Delta H_{\beta 4}^\circ$[d]	40.7 (5)	38.1 (4)	77 (3)	72.1 (5)
$\Delta S_{\beta 4}^\circ$[d]	419 (3)	414 (3)	400 (10)	380 (3)

[a] Values in parentheses are 3σ in the last significant digits. [b] 0.4 mol dm^{-3} $(C_2H_5)_4NClO_4$; ref 10. [c] This work (N = 151, σ_q = 0.019, R = 0.016). [d] For the overall formation of $[NiCl_4]^{2-}$.

Table IV. Peak Positions and Heights, λ_{max}/nm (ϵ_{max}/10 mol^{-1} dm^2), of Absorption Bands of Nickel(II) Chloro Complexes in *N,N*-Dimethylacetamide

	278 K	298 K	318 K
Ni^{2+}	424 (15)	427 (16)	429 (17)
	789 (5)	796 (5)	806 (5)
$[NiCl]^+$	459 (77)	461 (94)	463 (105)
$[NiCl_2]$	485 (52)	489 (40)	
	556 (73)	558 (82)	558 (87)
	595 (79)	598 (87)	597 (93)
$[NiCl_3]^-$	627 (161)	626 (158)	625 (156)
	678 (106)	682 (102)	684 (100)
$[NiCl_4]^{2-}$	658 (215)	658 (210)	656 (204)
	703 (224)	704 (217)	703 (211)

spline interpolation and summarized in Table IV. According to a recent EXAFS study,[24] the coordination number of Ni^{2+} is 5.9 ± 0.1 in DMA solution. The spectrum of the solvated Ni^{2+} ion is typical of the octahedral NiO_6 chromophore, and the observed absorption band at 427 nm has been assigned to a spin-allowed transition $^3A_{2g} \rightarrow {}^3T_{1g}(P)$.[3,4] It has been reported that this band becomes a little larger and shifts to a longer wavelength with temperature increase.[5] This is also seen in this work (Table IV), but only very slightly, which indicates that the octahedral structure is essentially intact in this temperature region.

Both $[NiCl_3]^-$ and $[NiCl_4]^{2-}$ show intense bands at 620–700 nm, which are characteristic of tetrahedral complexes.[3,25] The latter complex exhibits a spectrum almost identical to that of $[NiCl_4]^{2-}$ in DMF,[10] DMSO,[15] and MeCN,[16] which is consistent with its four-coordinate structure without any solvent molecules in the vicinity of the nickel(II) center.

For the tri- and tetrachloro complexes, decrease in the peak heights with increasing temperature is noticeable (Figure 2a). There are several possible origins of temperature dependence of spectral lines, e.g. variation of metal–ligand distances, symmetry lowering, vibrational and rotational couplings, and vibronic transition mechanisms.[3] In the present case, however, the examined temperature range is rather limited, so that these factors are likely to cause only minor changes in the spectra. Indeed, the overall oscillator strengths calculated by integration of the spectrum[26] are found to be almost equal at all the temperatures, differing only by 0.4–0.6%, for both complexes. Therefore, the structures of $[NiCl_3]^-$ and $[NiCl_4]^{2-}$ are primarily unchanged.

The spectrum of the monochloro complex (Figure 2b) cannot be assigned to either an octahedral or a tetrahedral geometry. The substantial increase in extinction coefficients and the major transition energy greater than 20 000 cm^{-1} exclude these coordination geometries for O- and Cl-donor ligands.[3,27] A four-coordinate square planar structure is also ruled out on the basis of the weak but appreciable absorption[3] above 800 nm and the absorption maximum of 461 nm, which is unlikely for the donor atom set O_3Cl; comparison can be made with a square planar complex $[Ni(Et_4dien)Cl]^+$ (531 nm; Et_4dien = 1,1,7,7-tetraethyldiethylenetriamine).[28] On the other hand, high-spin five-coordinate Ni^{II} complexes with weak-field ligands exhibit relatively intense absorption bands at wavelengths shorter than 500 nm, e.g., NiO_5 chromophores at 430–460 nm[29,30] and the NiN_4Cl chromophore at 429 nm.[31] An accompanying shoulder on the longer wavelength side is also typical of these complexes. Furthermore, there is a marked similarity between this spectrum and that of $[Ni(TMU)_5]^{2+}$ (TMU = 1,1,3,3-tetramethylurea).[32] Therefore, the spectrum is diagnostic of five-coordinate $[NiCl(DMA)_4]^+$.

Though many high-spin five-coordinate nickel(II) complexes have now been reported,[33,34] those with unidentate ligands are still very rare. A few instances are $[NiX(OAsMePh_2)_4]^+$ (X = NO_3, ClO_4)[29,30] and a series of complexes containing 1,4-diazabicyclo[2.2.2]octane derivatives.[35,36] All of these complexes contain bulky ligands, and the unusual coordination structure is probably due to the steric limitation to the attainment of six-coordination. As DMA molecules also cause steric crowding in $[Ni(DMA)_6]^{2+}$, coordination of the chloride ion may increase the repulsion between the ligating atoms, to form the five-coordinate $[NiCl(DMA)_4]^+$ complex. In the other solvents without such steric effects (DMF, DMSO, and MeCN), $[NiCl]^+$ shows a spectrum typical of six-coordinate octahedral complexes.[10,15,16]

The absorption of $[NiCl]^+$ at 461 nm becomes stronger with temperature increase. This change is so large that it points to an equilibrium between species with different geometries. Although the major component of the spectrum is assigned to the five-coordinate species, the monochloro complex is actually a mixture of different species, its spectrum being a superposition (weighted sum) of the constituents. In view of the absence of any isosbestic point, the other species may have weaker absorption bands (if any) which are hidden by the intense absorption of the major species. As an octahedral NiO_5Cl chromophore is expected to show a weak absorption above 430 nm,[10] an equilibrium between octahedral and five-coordinate complexes is likely:

$$[NiCl(DMA)_5]^+ \rightleftarrows [NiCl(DMA)_4]^+ + DMA \quad (6)$$

As temperature increases, the equilibrium shifts to the right-hand side.

(24) Ozutsumi, K.; Koide, M.; Suzuki, H.; Ishiguro, S. To be published.
(25) Gerloch, M.; Manning, M. R. *Inorg. Chem.* **1981**, *20*, 1051.
(26) Atkins, P. W. *Physical Chemistry*, 2nd ed.; Oxford University Press: Oxford, U.K., 1982.
(27) Rosenberg, R. C.; Root, C. A.; Gray, H. B. *J. Am. Chem. Soc.* **1975**, *97*, 21.
(28) Dori, Z.; Gray, H. B. *J. Am. Chem. Soc.* **1966**, *88*, 1394.
(29) Lions, F.; Dance, J. D.; Lewis, J. *J. Chem. Soc. A* **1967**, 565.
(30) Gerloch, M.; Kohl, J.; Lewis, J.; Urland, W. *J. Chem. Soc. A* **1970**, 3269.
(31) Ciampolini, M.; Nardi, N. *Inorg. Chem.* **1966**, *5*, 41.
(32) Inada, Y.; Ozutsumi, K.; Funahashi, S. *Proc. Symp. Solution Chem. Jpn.* **1991**, *14*, 174.
(33) Orioli, P. L. *Coord. Chem. Rev.* **1971**, *6*, 285.
(34) Ciampolini, M. *Struct. Bonding* **1969**, *6*, 52.
(35) Ross, F. K.; Stucky, G. D. *Inorg. Chem.* **1969**, *8*, 2734.
(36) Vallarino, L. M.; Goedken, V. L.; Quagliano, J. V. *Inorg. Chem.* **1972**, *11*, 1466.

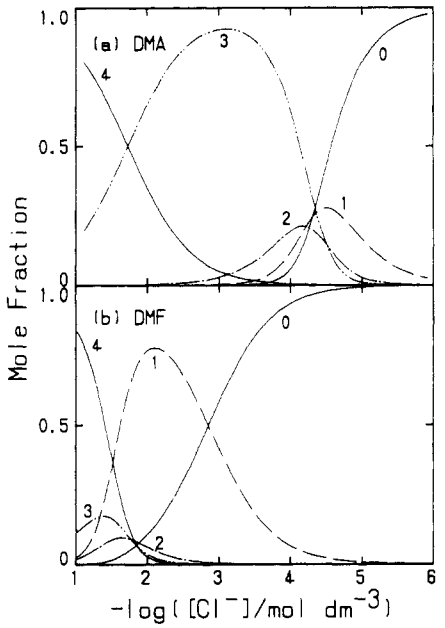

Figure 4. Distribution of the nickel(II) chloro complexes in DMA (a) and in DMF (b) at 298 K. The numbers represent n in $[NiCl_n]^{(2-n)+}$.

The dichloro complex has three distinct absorption peaks and also exhibits extensive thermochromism (Figure 2c). In this case, a clear isosbestic point is observed at 518 nm, indicating an equilibrium between two distinct species. The peak at 489 nm may be assigned to a five-coordinate species with a NiO_3Cl_2 chromophore, which corresponds to a lower energy (by 1200 cm^{-1}) than that of $[NiCl(DMA)_4]^+$. The spectrum above 518 nm, consisting of two peaks and a shoulder, is very similar to that of $[NiCl_3(DMA)]^-$; the band maxima are shifted to higher energies by ca. 2000 cm^{-1}, which is again consistent with the field strength order O > Cl. These lead to a conclusion that the following solvation equilibrium holds:

$$[NiCl_2(DMA)_3] \rightleftarrows [NiCl_2(DMA)_2]\ (T_d) + DMA \quad (7)$$

The temperature increase shifts this equilibrium to the right-hand side. In DMF, DMSO, and MeCN, the dichloro complex has an octahedral structure $[NiCl_2(solvent)_4]$.[10,15,16] Again, the unique coordination structures in DMA imply the significance of the steric hindrance of coordinating DMA molecules.

Thermodynamics of Complexation. Figure 4 shows the distribution of the complexes in DMA and in DMF.[10] $[NiCl]^+$ and $[NiCl_2]$ are minor complexes in DMA, whereas $[NiCl_2]$ and $[NiCl_3]^-$ are minor in DMF. The complexation in DMA is strongly favored over that in DMF, which is unexpected from similar solvent properties of the two. The greater stability is of enthalpic nature, as is seen from a large difference in $\Delta H^\circ_{\beta 4}$ in DMA and DMF (36 kJ mol^{-1}); the corresponding $\Delta S^\circ_{\beta 4}$ values are very similar (Table III). Therefore, much weaker solvation in DMA is probably the major reason for the favored complexation. Though the Ni–O bond length in $[Ni(DMA)_6]^{2+}$ is normal (205 ± 1 pm),[24] the acetyl methyl groups may severely restrict the orientation of coordinated DMA molecules and thus decrease the solvation energy (ligand-field[4] and ion–dipole interaction energies) of the metal ion. Increased lability of metal ions in DMA[5,37,38] indeed suggests decreased metal–DMA bond energies. Solvation of Cl^- is also weaker in DMA than in DMF, as is seen from the positive enthalpy of transfer of Cl^- from DMF to DMA (17.7 kJ mol^{-1}).[39]

The stepwise enthalpy and entropy are also very different in these solvents. In DMF, the ΔH°_3 and ΔS°_3 values are markedly larger than those for the other steps at both 298 and 318 K, which has been ascribed to an extensive liberation of DMF molecules due to the geometry change:[10]

$$[NiCl_2(DMF)_4] + Cl^- \rightarrow [NiCl_3(DMF)]^- + 3DMF \quad (8)$$

In DMA, however, the ΔH°_n and ΔS°_n values for n = 1 and 2 are both large and the ΔH°_3 and ΔS°_3 values are relatively small. The large enthalpies and entropies for the first two steps suggest that the geometry change and desolvation are predominant at these steps in DMA. This is consistent with the coordination structures (Scheme I); the monochloro complex is an equilibrated mixture of $[NiCl(DMA)_5]^+$ and $[NiCl(DMA)_4]^+$, and the dichloro complex is a mixture of $[NiCl_2(DMA)_3]$ and $[NiCl_2(DMA)_2]$. Accordingly, the desolvation due to the geometry change may mostly occur upon the formation of the mono- and dichloro complexes.

Scheme I. Solvation Equilibria of the Nickel(II) Chloro Complexes in DMA[a]

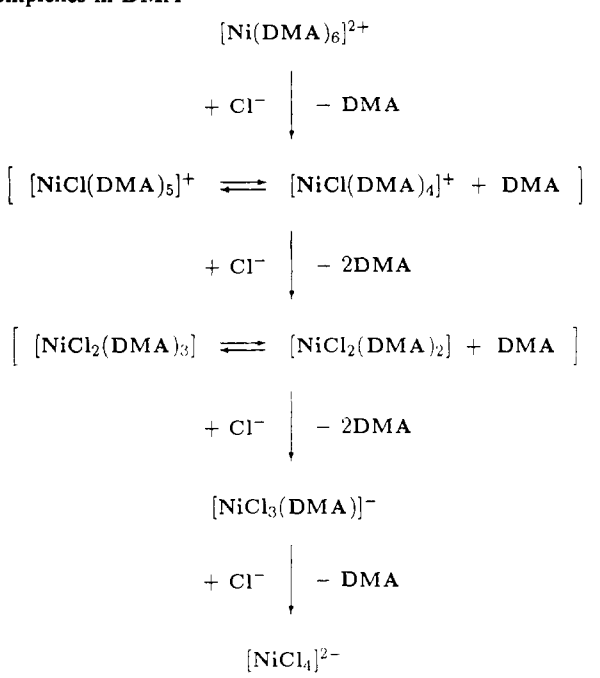

[a] Downward arrows denote complexation equilibria.

The comparison of thermodynamic parameters determined at 298 and 318 K in DMA (Table III) reveals that each step of complexation shows a different temperature dependence. As temperature increases, the stepwise formation constants log K_1 and log K_2 increase and log K_3 and log K_4 decrease. Enthalpy and entropy estimated from the temperature dependence of log K_n by the van't Hoff method[40] are only roughly in agreement with those obtained by calorimetry; the enthalpies and entropies are also temperature dependent. As temperature increases, the ΔH°_1 and ΔS°_1 values increase (by 4 kJ mol^{-1} and 14 J K^{-1} mol^{-1}), whereas the ΔH°_3 and ΔS°_3 values decrease (by 4.8 kJ mol^{-1} and 15 J K^{-1} mol^{-1}). On the other hand, the ΔH°_4 and ΔS°_4 values show little change. The temperature dependence of enthalpies and entropies is quantitatively described by introducing the molar heat capacity of a complex formation reaction at constant pressure[41] (Table V):

$$\Delta C^\circ_{pn} = (\partial \Delta H^\circ_n/\partial T)_p = T(\partial \Delta S^\circ_n/\partial T)_p \quad (9)$$

The values obtained from the enthalpies are in excellent agreement with the corresponding values from the entropies.

(37) Caminiti, R.; Crisponi, G.; Nurchi, V. *Z. Naturforsch.* **1984**, *39A*, 1235.
(38) Veselov, I. A.; Shtyrlin, V. G.; Zakharov, A. V. *Koord. Khim.* **1988**, *14*, 943; *Sov. J. Coord. Chem. (Engl. Transl.)* **1988**, *14*, 527.
(39) Marcus, Y.; Kamlet, M. J.; Taft, R. W. *J. Phys. Chem.* **1988**, *92*, 3613.
(40) Pitzer, K. S.; Brewer, L. *Thermodynamics*, 2nd ed.; McGraw-Hill: New York, 1961.
(41) Leffler, J. E.; Grunwald, E. *Rates and Equilibria of Organic Reactions*; Wiley: New York, 1963.

Table V. Molar Heat Capacities, ΔC°_{pn}/kJ K^{-1} mol^{-1}, for the Stepwise Formation Reaction of $[NiCl_n]^{(2-n)+}$ in *N,N*-Dimethylacetamide (DMA) and in *N,N*-Dimethylformamide (DMF) Estimated from the Enthalpy and Entropy Data at 298 and 318 K[a]

		from enthalpies	from entropies
in DMA	ΔC°_{p1}	0.20 (3)	0.22 (4)
	ΔC°_{p2}	−0.09 (6)	−0.05 (8)
	ΔC°_{p3}	−0.24 (4)	−0.23 (6)
	ΔC°_{p4}	−0.01 (3)	0.00 (2)
in DMF	ΔC°_{p1}	0.02 (3)	−0.02 (2)

[a] Values in parentheses are 3σ in the last significant digits.

In general, heat capacity of ions and complexes in solution has contributions from both intramolecular kinetic modes of motion (internal rotation and vibration) and intermolecular interactions (electrostatic interactions and liquid-state structure of the solvent). Since ΔC°_{pn} corresponds to the difference before and after complexation, the most important contributions are the ones which are sensitive to complexation, i.e., (i) intramolecular heat capacity accompanying the newly created or broken bonds and (ii) electrostatic (Born and Debye–Hückel) heat capacity which depends on the change in formal charges of complexes.[40] Compared with the values in Table V, the intramolecular contributions are small; for example, a one-dimensional classical rotator has $C_{rot} = 0.5R = 4.2$ J K^{-1} mol^{-1} and a harmonic oscillator with a wavenumber of 200 cm^{-1} has $C_{vib} = 0.93R = 7.7$ J K^{-1} mol^{-1} at 298 K.[40] The electrostatic terms are more difficult to evaluate, because good estimation for $\partial^2\epsilon/\partial T^2$ is necessary. Nevertheless, the ΔC°_{pn} values have no appreciable correlation with the change in formal charges, which implies that the electrostatic contributions may also be minor. It follows that a rather small value is usually expected for the ΔC°_{pn} values, unless there is an extra origin of heat capacity. This is indeed the case for ΔC°_{p4} in DMA and ΔC°_{p1} in DMF, which are both practically zero. No solvation equilibrium is involved in these reactions; in DMA the tri- and tetrachloro complexes both exist as four-coordinate species, and in DMF the nickel(II) ion and monochloro complex both exist as six-coordinate species.[10]

On the other hand, the positive value of ΔC°_{p1} and the negative value of ΔC°_{p3} are much more pronounced. This may be qualitatively explained by considering equilibria 6 and 7 discussed in the previous section. According to Le Chatelier's principle, an equilibrium shifts in the endothermic direction with increasing temperature; therefore, reactions 6 and 7 should both be endothermic. The presence of equilibrium 6 may have a large positive contribution to ΔC°_{p1}, because at a higher temperature the population of $[NiCl(DMA)_4]^+$ increases and an excess energy is required to produce this five-coordinate species. This has some analogy to the extraordinarily large heat capacity due to the first-order phase transition. On the contrary, the presence of equilibrium 7 may lead to a negative ΔC°_{p3}, because the initial state of this reaction consists of two species. At a higher temperature, the population of four-coordinate $[NiCl_2(DMA)_2]$ increases, and thus less energy is needed for formation of $[NiCl_3(DMA)]^-$.

An alternative, complementary interpretation of heat capacity is provided by statistical mechanics. According to the fluctuation–dissipation theorem, heat capacity is generally proportional to energy fluctuations (mean-square deviations from the average) in a canonical ensemble:

$$\langle (E - \langle E \rangle)^2 \rangle = RT^2 C_v \qquad (10)$$

where $\langle\ \rangle$ denotes ensemble average.[42] This equation indeed suggests that larger heat capacities may commonly be expected for complexes involving solvation equilibria, because energy fluctuates more greatly in an ensemble which is a mixture of two (or more) distinct species with different enthalpies than in one consisting of a single molecular structure.

Acknowledgment. This work was financially supported by Grants-in-Aid for Scientific Research (No. 2640469) and for Scientific Research in Priority Areas (No. 02245106) from the Ministry of Education, Science, and Culture of Japan. We thank K. Ozutsumi and Y. Inada for fruitful discussions of their recent results.

(42) Chandler, D. *Introduction of Modern Statistical Mechanics*; Oxford University Press: New York, 1987.